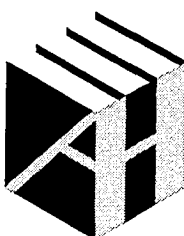


Computational Electrodynamics

The Finite-Difference Time-Domain Method

Third Edition

Allen Taflove
Susan C. Hagness



**ARTECH
HOUSE**

BOSTON | LONDON
artechhouse.com

Contents

Preface to the Third Edition	xix
1 Electrodynamics Entering the 21st Century	1
1.1 Introduction	1
1.2 The Heritage of Military Defense Applications	1
1.3 Frequency-Domain Solution Techniques	2
1.4 Rise of Finite-Difference Time-Domain Methods	3
1.5 History of FDTD Techniques for Maxwell's Equations	4
1.6 Characteristics of FDTD and Related Space-Grid Time-Domain Techniques	6
1.6.1 Classes of Algorithms	6
1.6.2 Predictive Dynamic Range	7
1.6.3 Scaling to Very Large Problem Sizes	8
1.7 Examples of Applications	9
1.7.1 Impulsive Around-the-World Extremely Low-Frequency Propagation	10
1.7.2 Cellphone Radiation Interacting with the Human Head	11
1.7.3 Early-Stage Detection of Breast Cancer Using an Ultrawideband Microwave Radar	11
1.7.4 Homing Accuracy of a Radar-Guided Missile	12
1.7.5 Electromagnetic Wave Vulnerabilities of a Military Jet Plane	12
1.7.6 Millimeter-Wave Propagation in a Defect-Mode Electromagnetic Bandgap Structure	13
1.7.7 Photonic Crystal Microcavity Laser	14
1.7.8 Photonic Crystal Cross-Waveguide Switch	15
1.8 Conclusions	16
References	16
2 The One-Dimensional Scalar Wave Equation	21
2.1 Introduction	21
2.2 Propagating-Wave Solutions	21
2.3 Dispersion Relation	22
2.4 Finite Differences	23
2.5 Finite-Difference Approximation of the Scalar Wave Equation	24
2.6 Numerical Dispersion Relation	27
2.6.1 Case 1: Very Fine Sampling in Time and Space	28
2.6.2 Case 2: Magic Time-Step	29
2.6.3 Case 3: Dispersive Wave Propagation	29
2.6.4 Example of Calculation of Numerical Phase Velocity and Attenuation	34
2.6.5 Examples of Calculations of Pulse Propagation	34
2.7 Numerical Stability	39
2.7.1 Complex-Frequency Analysis	40
2.7.2 Examples of Calculations Involving Numerical Instability	43
2.8 Summary	45
Appendix 2A: Order of Accuracy	47
2A.1 Lax-Richtmyer Equivalence Theorem	47
2A.2 Limitations	48
References	48
Selected Bibliography on Stability of Finite-Difference Methods	49
Problems	49

3 Introduction to Maxwell's Equations and the Yee Algorithm

Allen Taflove and Jamesina Simpson

3.1	Introduction	51
3.2	Maxwell's Equations in Three Dimensions	51
3.3	Reduction to Two Dimensions	54
3.3.1	TM_z Mode	55
3.3.2	TE_z Mode	55
3.4	Reduction to One Dimension	56
3.4.1	x -Directed, z -Polarized TEM Mode	56
3.4.2	x -Directed, y -Polarized TEM Mode	57
3.5	Equivalence to the Wave Equation in One Dimension	57
3.6	The Yee Algorithm	58
3.6.1	Basic Ideas	58
3.6.2	Finite Differences and Notation	60
3.6.3	Finite-Difference Expressions for Maxwell's Equations in Three Dimensions	62
3.6.4	Space Region with a Continuous Variation of Material Properties	67
3.6.5	Space Region with a Finite Number of Distinct Media	69
3.6.6	Space Region with Nonpermeable Media	71
3.6.7	Reduction to the Two-Dimensional TM_z and TE_z Modes	73
3.6.8	Interpretation as Faraday's and Ampere's Laws in Integral Form	75
3.6.9	Divergence-Free Nature	78
3.7	Alternative Finite-Difference Grids	80
3.7.1	Cartesian Grids	80
3.7.2	Hexagonal Grids	82
3.8	Emerging Application: Gridding the Planet Earth	85
3.8.1	Background	85
3.8.2	The Latitude-Longitude Space Lattice	86
3.8.3	The Geodesic (Hexagon-Pentagon) Grid	99
3.9	Summary	103
	References	104
	Problems	105

4 Numerical Dispersion and Stability

4.1	Introduction	107
4.2	Derivation of the Numerical Dispersion Relation for Two-Dimensional Wave Propagation	107
4.3	Extension to Three Dimensions	110
4.4	Comparison with the Ideal Dispersion Case	111
4.5	Anisotropy of the Numerical Phase Velocity	111
4.5.1	Sample Values of Numerical Phase Velocity	111
4.5.2	Intrinsic Grid Velocity Anisotropy	116
4.6	Complex-Valued Numerical Wavenumbers	120
4.6.1	Case 1: Numerical Wave Propagation Along the Principal Lattice Axes	121
4.6.2	Numerical Wave Propagation Along a Grid Diagonal	123
4.6.3	Example of Calculation of Numerical Phase Velocity and Attenuation	126
4.6.4	Example of Calculation of Wave Propagation	126
4.7	Numerical Stability	128
4.7.1	Complex-Frequency Analysis	130
4.7.2	Example of a Numerically Unstable Two-Dimensional FDTD Model	135
4.7.3	Linear Growth Mode When the Normalized Courant Factor Equals 1	137
4.8	Generalized Stability Problem	137
4.8.1	Absorbing and Impedance Boundary Conditions	137

4.8.2	Variable and Unstructured Meshing	137
4.8.3	Lossy, Dispersive, Nonlinear, and Gain Materials	138
4.9	Modified Yee-Based Algorithms for Mitigating Numerical Dispersion	138
4.9.1	Strategy 1: Center a Specific Numerical Phase-Velocity Curve About c	138
4.9.2	Strategy 2: Use Fourth-Order-Accurate Explicit Spatial Differences	139
4.9.3	Strategy 3: Use a Hexagonal Grid, If Possible	146
4.9.4	Strategy 4: Use Discrete Fourier Transforms to Calculate the Spatial Derivatives	150
4.10	Alternating-Direction-Implicit Time-Stepping Algorithm for Operation Beyond the Courant Limit	154
4.10.1	Numerical Formulation of the Zheng/Chen/Zhang Algorithm	155
4.10.2	Sources	161
4.10.3	Numerical Stability	161
4.10.4	Numerical Dispersion	163
4.10.5	Additional Accuracy Limitations and Their Implications	164
4.11	Summary	164
	References	165
	Problems	166
	Projects	167

5 Incident Wave Source Conditions

Allen Taflove, Geoff Waldschmidt, Christopher Wagner, John Schneider, and Susan Hagness **169**

5.1	Introduction	169
5.2	Pointwise \mathbf{E} and \mathbf{H} Hard Sources in One Dimension	169
5.3	Pointwise \mathbf{E} and \mathbf{H} Hard Sources in Two Dimensions	171
5.3.1	Green Function for the Scalar Wave Equation in Two Dimensions	171
5.3.2	Obtaining Comparative FDTD Data	172
5.3.3	Results for Effective Action Radius of a Hard-Sourced Field Component	173
5.4	\mathbf{J} and \mathbf{M} Current Sources in Three Dimensions	175
5.4.1	Sources and Charging	176
5.4.2	Sinusoidal Sources	178
5.4.3	Transient (Pulse) Sources	178
5.4.4	Intrinsic Lattice Capacitance	179
5.4.5	Intrinsic Lattice Inductance	183
5.4.6	Impact upon FDTD Simulations of Lumped-Element Capacitors and Inductors	183
5.5	The Plane-Wave Source Condition	185
5.6	The Total-Field / Scattered-Field Technique: Ideas and One-Dimensional Formulation	186
5.6.1	Ideas	186
5.6.2	One-Dimensional Formulation	188
5.7	Two-Dimensional Formulation of the TF/SF Technique	193
5.7.1	Consistency Conditions	193
5.7.2	Calculation of the Incident Field	197
5.7.3	Illustrative Example	201
5.8	Three-Dimensional Formulation of the TF/SF Technique	204
5.8.1	Consistency Conditions	204
5.8.2	Calculation of the Incident Field	210
5.9	Advanced Dispersion Compensation in the TF/SF Technique	213
5.9.1	Matched Numerical Dispersion Technique	214
5.9.2	Analytical Field Propagation	218
5.10	Scattered-Field Formulation	220
5.10.1	Application to PEC Structures	220
5.10.2	Application to Lossy Dielectric Structures	221
5.10.3	Choice of Incident Plane-Wave Formulation	223

5.11 Waveguide Source Conditions	223
5.11.1 Pulsed Electric Field Modal Hard Source	223
5.11.2 Total-Field / Reflected-Field Modal Formulation	225
5.11.3 Resistive Source and Load Conditions	225
5.12 Summary	226
References	227
Problems	227
Projects	228
6 Analytical Absorbing Boundary Conditions	229
6.1 Introduction	229
6.2 Bayliss-Turkel Radiation Operators	230
6.2.1 Spherical Coordinates	231
6.2.2 Cylindrical Coordinates	234
6.3 Engquist-Majda One-Way Wave Equations	236
6.3.1 One-Term and Two-Term Taylor Series Approximations	237
6.3.2 Mur Finite-Difference Scheme	240
6.3.3 Trefethen-Halpern Generalized and Higher-Order ABCs	243
6.3.4 Theoretical Reflection Coefficient Analysis	245
6.3.5 Numerical Experiments	247
6.4 Higdon Radiation Operators	252
6.4.1 Formulation	252
6.4.2 First Two Higdon Operators	253
6.4.3 Discussion	254
6.5 Liao Extrapolation in Space and Time	255
6.5.1 Formulation	255
6.5.2 Discussion	257
6.6 Ramahi Complementary Operators	259
6.6.1 Basic Idea	259
6.6.2 Complementary Operators	260
6.6.3 Effect of Multiple Wave Reflections	260
6.6.4 Basis of the Concurrent Complementary Operator Method	261
6.6.5 Illustrative FDTD Modeling Results Obtained Using the C-COM	267
6.7 Summary	270
References	270
Problems	271
7 Perfectly Matched Layer Absorbing Boundary Conditions	273
<i>Stephen Gedney</i>	
7.1 Introduction	273
7.2 Plane Wave Incident upon a Lossy Half-Space	274
7.3 Plane Wave Incident upon Berenger's PML Medium	276
7.3.1 Two-Dimensional TE_z Case	276
7.3.2 Two-Dimensional TM_z Case	281
7.3.3 Three-Dimensional Case	281
7.4 Stretched-Coordinate Formulation of Berenger's PML	282
7.5 An Anisotropic PML Absorbing Medium	285
7.5.1 Perfectly Matched Uniaxial Medium	285
7.5.2 Relationship to Berenger's Split-Field PML	288
7.5.3 A Generalized Three-Dimensional Formulation	289
7.5.4 Inhomogeneous Media	290

7.6	Theoretical Performance of the PML	291
7.6.1	The Continuous Space	291
7.6.2	The Discrete Space	292
7.7	Complex Frequency-Shifted Tensor	294
7.7.1	Introduction	294
7.7.2	Strategy to Reduce Late-Time (Low-Frequency) Reflections	296
7.8	Efficient Implementation of UPML in FDTD	297
7.8.1	Derivation of the Finite-Difference Expressions	298
7.8.2	Computer Implementation of the UPML	301
7.9	Efficient Implementation of CPML in FDTD	302
7.9.1	Derivation of the Finite-Difference Expressions	302
7.9.2	Computer Implementation of the CPML	307
7.10	Application of CPML in FDTD to General Media	310
7.10.1	Introduction	310
7.10.2	Example: Application of CPML to the Debye Medium	310
7.11	Numerical Experiments with PML	313
7.11.1	Current Source Radiating in an Unbounded Two-Dimensional Region	313
7.11.2	Highly Elongated Domains and Edge Singularities	317
7.11.3	Microstrip Patch Antenna Array	320
7.11.4	Dispersive Media	322
7.12	Summary and Conclusions	324
	References	324
	Projects	327
8	Near-to-Far-Field Transformation	
	<i>Allen Tafløe, Xu Li, and Susan Hagness</i>	329
8.1	Introduction	329
8.2	Two-Dimensional Transformation, Phasor Domain	329
8.2.1	Application of Green's Theorem	330
8.2.2	Far-Field Limit	332
8.2.3	Reduction to Standard Form	334
8.3	Obtaining Phasor Quantities Via Discrete Fourier Transformation	335
8.4	Surface Equivalence Theorem	338
8.5	Extension to Three Dimensions, Phasor Domain	340
8.6	Time-Domain Near-to-Far-Field Transformation	343
8.7	Modified NTFF Procedure to More Accurately Calculate Backscattering from Strongly Forward-Scattering Objects	348
8.8	Summary	351
	References	351
	Project	352
9	Dispersive, Nonlinear, and Gain Materials	
	<i>Allen Tafløe, Susan Hagness, Wojciech Gwarek, Masafumi Fujii, and Shih-Hui Chang</i>	353
9.1	Introduction	353
9.2	Generic Isotropic Material Dispersions	354
9.2.1	Debye Media	354
9.2.2	Lorentz Media	354
9.2.3	Drude Media	355
9.3	Piecewise-Linear Recursive-Convolution Method, Linear Material Case	355
9.3.1	General Formulation	356
9.3.2	Application to Debye Media	358

9.3.3 Application to Lorentz Media	358
9.3.4 Numerical Results	360
9.4 Auxiliary Differential Equation Method, Linear Material Case	361
9.4.1 Formulation for Multiple Debye Poles	361
9.4.2 Formulation for Multiple Lorentz Pole Pairs	363
9.4.3 Formulation for Multiple Drude Poles	365
9.4.4 Illustrative Numerical Results	367
9.5 Modeling of Linear Magnetized Ferrites	369
9.5.1 Equivalent RLC Model	370
9.5.2 Time-Stepping Algorithm	371
9.5.3 Extension to the Three-Dimensional Case, Including Loss	373
9.5.4 Illustrative Numerical Results	374
9.5.5 Comparison of Computer Resources	375
9.6 Auxiliary Differential Equation Method, Nonlinear Dispersive Material Case	376
9.6.1 Strategy	376
9.6.2 Contribution of the Linear Debye Polarization	377
9.6.3 Contribution of the Linear Lorentz Polarization	377
9.6.4 Contributions of the Third-Order Nonlinear Polarization	378
9.6.5 Electric Field Update	380
9.6.6 Illustrative Numerical Results for Temporal Solitons	381
9.6.7 Illustrative Numerical Results for Spatial Solitons	383
9.7 Auxiliary Differential Equation Method, Macroscopic Modeling of Saturable, Dispersive Optical Gain Materials	387
9.7.1 Theory	387
9.7.2 Validation Studies	390
9.8 Auxiliary Differential Equation Method, Modeling of Lasing Action in a Four-Level Two-Electron Atomic System	394
9.8.1 Quantum Physics Basis	394
9.8.2 Coupling to Maxwell's Equations	398
9.8.3 Time-Stepping Algorithm	398
9.8.4 Illustrative Results	400
9.9 Summary and Conclusions	402
References	404
Problems	405
Projects	406

10 Local Subcell Models of Fine Geometrical Features

Allen Taflove, Małgorzata Celuch-Marcysiak, and Susan Hagness

407

10.1 Introduction	407
10.2 Basis of Contour-Path FDTD Modeling	408
10.3 The Simplest Contour-Path Subcell Models	408
10.3.1 Diagonal Split-Cell Model for PEC Surfaces	410
10.3.2 Average Properties Model for Material Surfaces	410
10.4 The Contour-Path Model of the Narrow Slot	411
10.5 The Contour-Path Model of the Thin Wire	415
10.6 Locally Conformal Models of Curved Surfaces	420
10.6.1 Yu-Mittra Technique for PEC Structures	420
10.6.2 Illustrative Results for PEC Structures	421
10.6.3 Yu-Mittra Technique for Material Structures	424
10.7 Maloney-Smith Technique for Thin Material Sheets	427
10.7.1 Basis	427
10.7.2 Illustrative Results	430

10.8	Surface Impedance	432
10.8.1	The Monochromatic SIBC	434
10.8.2	Convolution-Based Models of the Frequency-Dependent SIBC	436
10.8.3	Equivalent-Circuit Model of the Frequency-Dependent SIBC	442
10.8.4	Sources of Error	445
10.8.5	Discussion	446
10.9	Thin Coatings on a PEC Surface	447
10.9.1	Method of Lee et al.	447
10.9.2	Method of Kärkkäinen	450
10.10	Relativistic Motion of PEC Boundaries	450
10.10.1	Basis	451
10.10.2	Illustrative Results	454
10.11	Summary and Discussion	458
	References	458
	Selected Bibliography	460
	Projects	461
11	Nonuniform Grids, Nonorthogonal Grids, Unstructured Grids, and Subgrids	
	<i>Stephen Gedney, Faiza Lansing, and Nicolas Chavannes</i>	463
11.1	Introduction	463
11.2	Nonuniform Orthogonal Grids	464
11.3	Locally Conformal Grids, Globally Orthogonal	471
11.4	Global Curvilinear Coordinates	471
11.4.1	Nonorthogonal Curvilinear FDTD Algorithm	471
11.4.2	Stability Criterion	477
11.5	Irregular Nonorthogonal Structured Grids	480
11.6	Irregular Nonorthogonal Unstructured Grids	486
11.6.1	Generalized Yee Algorithm	487
11.6.2	Inhomogeneous Media	491
11.6.3	Practical Implementation of the Generalized Yee Algorithm	493
11.7	A Planar Generalized Yee Algorithm	494
11.7.1	Time-Stepping Expressions	495
11.7.2	Projection Operators	496
11.7.3	Efficient Time-Stepping Implementation	498
11.7.4	Modeling Example: 32-GHz Wilkinson Power Divider	499
11.8	Cartesian Subgrids	501
11.8.1	Geometry	502
11.8.2	Time-Stepping Scheme	503
11.8.3	Spatial Interpolation	504
11.8.4	Numerical Stability Considerations	505
11.8.5	Reflection from the Interface of the Primary Grid and Subgrid	505
11.8.6	Illustrative Results: Helical Antenna on Generic Cellphone at 900 MHz	508
11.8.7	Computational Efficiency	510
11.9	Summary and Conclusions	510
	References	511
	Problems	514
	Projects	515

12 Bodies of Revolution

Thomas Jurgens, Jeffrey Blaschak, and Gregory Saewert

12.1 Introduction	517
12.2 Field Expansion	517
12.3 Difference Equations for Off-Axis Cells	519
12.3.1 Ampere's Law Contour Path Integral to Calculate e_r	519
12.3.2 Ampere's Law Contour Path Integral to Calculate e_ϕ	521
12.3.3 Ampere's Law Contour Path Integral to Calculate e_z	523
12.3.4 Difference Equations	525
12.3.5 Surface-Conforming Contour Path Integrals	528
12.4 Difference Equations for On-Axis Cells	529
12.4.1 Ampere's Law Contour Path Integral to Calculate e_z on the z-Axis	529
12.4.2 Ampere's Law Contour Path Integral to Calculate e_ϕ on the z-Axis	532
12.4.3 Faraday's Law Calculation of h_r on the z-Axis	534
12.5 Numerical Stability	535
12.6 PML Absorbing Boundary Condition	536
12.6.1 BOR-FDTD Background	536
12.6.2 Extension of PML to the General BOR Case	537
12.6.3 Examples	543
12.7 Application to Particle Accelerator Physics	543
12.7.1 Definitions and Concepts	545
12.7.2 Examples	547
12.8 Summary	550
References	550
Problems	551
Projects	552

13 Periodic Structures

James Maloney and Morris Kesler

13.1 Introduction	553
13.2 Review of Scattering from Periodic Structures	555
13.3 Direct Field Methods	559
13.3.1 Normal Incidence Case	559
13.3.2 Multiple Unit Cells for Oblique Incidence	560
13.3.3 Sine-Cosine Method	562
13.3.4 Angled-Update Method	563
13.4 Introduction to the Field-Transformation Technique	567
13.5 Multiple-Grid Approach	571
13.5.1 Formulation	571
13.5.2 Numerical Stability Analysis	573
13.5.3 Numerical Dispersion Analysis	574
13.5.4 Lossy Materials	575
13.5.5 Lossy Screen Example	577
13.6 Split-Field Method, Two Dimensions	578
13.6.1 Formulation	578
13.6.2 Numerical Stability Analysis	580
13.6.3 Numerical Dispersion Analysis	581
13.6.4 Lossy Materials	582
13.6.5 Lossy Screen Example	583

13.7 Split-Field Method, Three Dimensions	583
13.7.1 Formulation	584
13.7.2 Numerical Stability Analysis	589
13.7.3 UPML Absorbing Boundary Condition	590
13.8 Application of the Periodic FDTD Method	594
13.8.1 Electromagnetic Bandgap Structures	595
13.8.2 Frequency-Selective Surfaces	597
13.8.3 Antenna Arrays	597
13.9 Summary and Conclusions	603
Acknowledgments	603
References	603
Projects	605

14 Antennas

<i>James Maloney, Glenn Smith, Eric Thiele, Om Gandhi, Nicolas Chavannes, and Susan Hagness</i>	607
14.1 Introduction	607
14.2 Formulation of the Antenna Problem	607
14.2.1 Transmitting Antenna	607
14.2.2 Receiving Antenna	609
14.2.3 Symmetry	610
14.2.4 Excitation	611
14.3 Antenna Feed Models	612
14.3.1 Detailed Modeling of the Feed	613
14.3.2 Simple Gap Feed Model for a Monopole Antenna	614
14.3.3 Improved Simple Feed Model	617
14.4 Near-to-Far-Field Transformations	621
14.4.1 Use of Symmetry	621
14.4.2 Time-Domain Near-to-Far-Field Transformation	622
14.4.3 Frequency-Domain Near-to-Far-Field Transformation	624
14.5 Plane-Wave Source	625
14.5.1 Effect of an Incremental Displacement of the Surface Currents	625
14.5.2 Effect of an Incremental Time Shift	627
14.5.3 Relation to Total-Field / Scattered-Field Lattice Zoning	628
14.6 Case Study I: The Standard-Gain Horn	628
14.7 Case Study II: The Vivaldi Slotline Array	634
14.7.1 Background	634
14.7.2 The Planar Element	635
14.7.3 The Vivaldi Pair	637
14.7.4 The Vivaldi Quad	639
14.7.5 The Linear Phased Array	640
14.7.6 Phased-Array Radiation Characteristics Indicated by the FDTD Modeling	641
14.7.7 Active Impedance of the Phased Array	644
14.8 Near-Field Simulations	647
14.8.1 Generic 900-MHz Cellphone Handset in Free Space	647
14.8.2 900-MHz Dipole Antenna Near a Layered Bone-Brain Half-Space	649
14.8.3 840-MHz Dipole Antenna Near a Rectangular Brain Phantom	650
14.8.4 900-MHz Infinitesimal Dipole Antenna Near a Spherical Brain Phantom	650
14.8.5 1.9-GHz Half-Wavelength Dipole Near a Spherical Brain Phantom	652
14.9 Case Study III: The Motorola T250 Tri-Band Phone	653
14.9.1 FDTD Phone Model	654
14.9.2 Measurement Procedures	656
14.9.3 Free-Space Near-Field Investigations and Assessment of Design Capabilities	656

14.9.4 Performance in Loaded Conditions (SAM and MRI-Based Human Head Model)	657
14.9.5 Radiation Performance in Free Space and Adjacent to the SAM Head	659
14.9.6 Computational Requirements	661
14.9.7 Overall Assessment	661
14.10 Selected Additional Applications	661
14.10.1 Use of Electromagnetic Bandgap Materials	662
14.10.2 Ground-Penetrating Radar	663
14.10.3 Antenna-Radome Interaction	667
14.10.4 Biomedical Applications of Antennas	669
14.11 Summary and Conclusions	671
References	671
Projects	676
15 High-Speed Electronic Circuits with Active and Nonlinear Components	
<i>Melinda Piket-May, Wojciech Gwarek, Tzong-Lin Wu, Bijan Houshmand, Tatsuo Itoh, and Jamesina Simpson</i>	677
15.1 Introduction	677
15.2 Basic Circuit Parameters for TEM Striplines and Microstrips	679
15.2.1 Transmission Line Parameters	679
15.2.2 Impedance	680
15.2.3 S-Parameters	680
15.2.4 Differential Capacitance	681
15.2.5 Differential Inductance	682
15.3 Lumped Inductance Due to a Discontinuity	682
15.3.1 Flux / Current Definition	684
15.3.2 Fitting $Z(\omega)$ or $S(\omega)$ to an Equivalent Circuit	684
15.3.3 Discussion: Choice of Methods	685
15.4 Inductance of Complex Power-Distribution Systems	685
15.4.1 Method Description	685
15.4.2 Example: Multiplane Meshed Printed-Circuit Board	687
15.4.3 Discussion	688
15.5 Parallel Coplanar Microstrips	688
15.6 Multilayered Interconnect Modeling	690
15.7 S-Parameter Extraction for General Waveguides	692
15.8 Digital Signal Processing and Spectrum Estimation	694
15.8.1 Prony's Method	695
15.8.2 Autoregressive Models	697
15.8.3 Padé Approximation	702
15.9 Modeling of Lumped Circuit Elements	706
15.9.1 FDTD Formulation Extended to Circuit Elements	706
15.9.2 The Resistor	708
15.9.3 The Resistive Voltage Source	708
15.9.4 The Capacitor	709
15.9.5 The Inductor	711
15.9.6 The Arbitrary Two-Terminal Linear Lumped Network	711
15.9.7 The Diode	714
15.9.8 The Bipolar Junction Transistor	715
15.10 Direct Linking of FDTD and SPICE	717
15.10.1 Basic Idea	718
15.10.2 Norton Equivalent Circuit "Looking Into" the FDTD Space Lattice	719
15.10.3 Thevenin Equivalent Circuit "Looking Into" the FDTD Space Lattice	721

15.11	Case Study: A 6-GHz MESFET Amplifier Model	723
15.11.1	Large-Signal Nonlinear Model	723
15.11.2	Amplifier Configuration	725
15.11.3	Analysis of the Circuit without the Packaging Structure	726
15.11.4	Analysis of the Circuit with the Packaging Structure	728
15.12	Emerging Topic: Wireless High-Speed Digital Interconnects Using Defect-Mode Electromagnetic Bandgap Waveguides	731
15.12.1	Stopband of the Defect-Free Two-Dimensional EBG Structure	732
15.12.2	Passband of the Two-Dimensional EBG Structure with Waveguiding Defect	732
15.12.3	Laboratory Experiments and Supporting FDTD Modeling	734
15.13	Summary and Conclusions	736
	Acknowledgments	737
	References	737
	Selected Bibliography	740
	Projects	741

16 Photonics

Geoffrey Burr, Susan Hagness, and Allen Taflove **743**

16.1	Introduction	743
16.2	Introduction to Index-Contrast Guided-Wave Structures	743
16.3	FDTD Modeling Issues	744
16.3.1	Optical Waveguides	744
16.3.2	Material Dispersion and Nonlinearities	747
16.4	Laterally Coupled Microcavity Ring Resonators	747
16.4.1	Modeling Considerations: Two-Dimensional FDTD Simulations	748
16.4.2	Coupling to Straight Waveguides	750
16.4.3	Coupling to Curved Waveguides	750
16.4.4	Elongated Ring Designs ("Racetracks")	752
16.4.5	Resonances of the Circular Ring	752
16.5	Laterally Coupled Microcavity Disk Resonators	756
16.5.1	Resonances	756
16.5.2	Suppression of Higher-Order Radial Whispering-Gallery Modes	760
16.6	Vertically Coupled Racetrack	761
16.7	Introduction to Distributed Bragg Reflector Devices	765
16.8	Application to Vertical-Cavity Surface-Emitting Lasers	765
16.8.1	Passive Studies	766
16.8.2	Active Studies: Application of the Classical Gain Model	767
16.8.3	Application of a New Semiclassical Gain Model	769
16.9	Quasi-One-Dimensional DBR Structures	770
16.10	Introduction to Photonic Crystals	772
16.11	Calculation of Band Structure	774
16.11.1	The "Order-N" Method	775
16.11.2	Frequency Resolution	778
16.11.3	Filter Diagonalization Method	780
16.11.4	The Triangular Photonic Crystal Lattice	782
16.11.5	Sources of Error and Their Mitigation	784
16.12	Calculation of Mode Patterns	787
16.13	Variational Approach	790
16.14	Modeling of Defect-Mode Photonic Crystal Waveguides	791
16.14.1	Band Diagram of a Photonic Crystal Slab	793
16.14.2	Band Diagram of a Photonic Crystal Waveguide	795

16.14.3	Intrinsic Loss in Photonic Crystal Waveguides	798
16.14.4	Transmission in Photonic Crystal Waveguides	803
16.14.5	Aperiodic Photonic-Crystal Waveguides	806
16.14.6	Photonic Crystal Waveguide Extrinsic Scattering Loss from the Green Function	806
16.15	Modeling of Photonic Crystal Resonators	807
16.16	Modeling Examples of Photonic Crystal Resonators	810
16.16.1	Electrically Driven Microcavity Laser	810
16.16.2	Photonic Crystal Cross-Waveguide Switch	812
16.17	Introduction to Frequency Conversion in Second-Order Nonlinear Optical Materials	813
16.18	PSTD-4 Algorithm	813
16.19	Extension to Second-Order Nonlinear Media	814
16.20	Application to a Nonlinear Waveguide with a QPM Grating	814
16.21	Application to Nonlinear Photonic Crystals	817
16.22	Introduction to Nanoplasmonic Devices	820
16.23	FDTD Modeling Considerations	820
16.24	FDTD Modeling Applications	821
16.25	Introduction to Biophotonics	822
16.26	FDTD Modeling Applications	822
16.26.1	Vertebrate Retinal Rod	822
16.26.2	Precancerous Cervical Cells	824
16.26.3	Sensitivity of Backscattering Signatures to Nanometer-Scale Cellular Changes	827
16.27	PSTD Modeling Application to Tissue Optics	828
16.28	Summary	830
	Acknowledgments	830
	References	830

17 Advances in PSTD Techniques

Qing Liu and Gang Zhao

17.1	Introduction	847
17.2	Approximation of Derivatives	847
17.2.1	Derivative Matrix for the Second-Order Finite-Difference Method	848
17.2.2	Derivative Matrices for Fourth-Order and N 'th-Order Finite-Difference Methods	849
17.2.3	Trigonometric Interpolation and FFT Method	850
17.2.4	Nonperiodic Functions and Chebyshev Method	851
17.3	Single-Domain Fourier PSTD Method	854
17.3.1	Approximation of Spatial Derivatives	855
17.3.2	Numerical Stability and Dispersion	856
17.4	Single-Domain Chebyshev PSTD Method	857
17.4.1	Spatial and Temporal Grids	857
17.4.2	Maxwell's Equations in Curvilinear Coordinates	858
17.4.3	Spatial Derivatives	860
17.4.4	Time-Integration Scheme	861
17.5	Multidomain Chebyshev PSTD Method	861
17.5.1	Subdomain Spatial Derivatives and Time Integration	862
17.5.2	Subdomain Patching by Characteristics	863
17.5.3	Subdomain Patching by Physical Conditions	864
17.5.4	Filter Design for Corner Singularities	864
17.5.5	Multidomain PSTD Results for 2.5-Dimensional Problems	866
17.5.6	Multidomain PSTD Results for Three-Dimensional Problems	868
17.6	Penalty Method for Multidomain PSTD Algorithm	868

17.7	Discontinuous Galerkin Method for PSTD Boundary Patching	873
17.7.1	Weak Form of Maxwell's Equations	873
17.7.2	Space Discretization and Domain Transformation	873
17.7.3	Mass Matrix and Stiffness Matrix	874
17.7.4	Flux on the Boundary	876
17.7.5	Numerical Results for DG-PSTD Method	876
17.8	Summary and Conclusions	879
Appendix 17A: Coefficients for the Five-Stage, Fourth-Order Runge-Kutta Method		879
References		880
18	Advances in Unconditionally Stable Techniques	883
<i>Hans De Raedt</i>		
18.1	Introduction	883
18.2	General Framework	883
18.3	Matrix-Exponential Concepts	884
18.4	Product-Formula Approach	887
18.4.1	The Classic Yee Algorithm as a Particular Realization	887
18.4.2	The ADI Method as a Second Realization	888
18.4.3	Unconditionally Stable Algorithms: Real-Space Approach	889
18.4.4	Unconditionally Stable Algorithms: Fourier-Space Approach	891
18.5	Chebyshev Polynomial Algorithm	892
18.6	Extension to Linear Dispersive Media	895
18.7	Extension to Perfectly Matched Layer Absorbing Boundary Conditions	898
18.8	Summary	899
Appendix 18A: Some Technical Details		900
Appendix 18B: Stability Analysis of Equation (18.17)		902
Appendix 18C: Stability Analysis of Equation (18.19)		904
References		904
Projects		905
19	Advances in Hybrid FDTD-FE Techniques	907
<i>Thomas Rylander, Fredrik Edelvik, Anders Bondeson, and Douglas Riley</i>		
19.1	Introduction	907
19.2	Time-Domain Finite Elements	910
19.2.1	Coupled Curl Equations	910
19.2.2	Wave Equation	913
19.2.3	Equivalences Between Finite Elements and FDTD	917
19.3	Tetrahedral, Hexahedral (Brick), and Pyramidal Zeroth-Order Edge and Facet Elements	918
19.3.1	Tetrahedral Finite Elements	919
19.3.2	Hexahedral (Brick) Finite Elements	921
19.3.3	Pyramidal Finite Elements	922
19.4	Stable Hybrid FDTD-FE Interface	924
19.4.1	Spatial Discretization	924
19.4.2	Time-Stepping on a Hybrid Space Lattice	927
19.4.3	Generalized Newmark Scheme	928
19.4.4	Proof of Stability	929
19.4.5	Alternative Time-Stepping Schemes	930
19.4.6	Extensions of the Hybrid FDTD-FE Concept	931
19.4.7	Reflection at the Interface of FDTD and FE Regions of a Hybrid Space Lattice	931
19.4.8	Scattering from the PEC Sphere	933
19.5	Mesh-Generation Approaches	935

19.6	Subcell Wire and Slot Algorithms for Time-Domain Finite Elements	936
19.6.1	Modeling Thin Wires	936
19.6.2	Modeling Thin Slots	939
19.6.3	Numerical Results for Thin Wires and Slots	941
19.7	Application to Advanced Scattering and Radiation Problems	943
19.7.1	Monostatic RCS of the NASA Almond	943
19.7.2	Bistatic RCS of the Saab <i>Trainer</i> Aircraft	945
19.7.3	Input Impedance of the Four-Arm Sinuous Antenna	948
19.8	Summary	949
	Acknowledgments	950
	References	950
20	Advances in Hardware Acceleration for FDTD	
	<i>Ryan Schneider, Sean Krakiwsky, Laurence Turner, and Michal Okoniewski</i>	955
20.1	Introduction	955
20.2	Background Literature	956
20.3	Fundamental Design Considerations	957
20.4	Conceptual Massively Parallel FPGA Implementation	958
20.5	Case Study of Using the FPGA as a Coprocessor	962
20.6	Performance of Custom Hardware Implementations	964
20.7	Fundamentals of Graphics Processor Units	965
20.7.1	Overview	965
20.7.2	Graphics Pipeline	965
20.7.3	Memory Interface	967
20.7.4	Programmable Fragment and Vertex Processors	968
20.8	Implementing FDTD on a Graphics Processor Unit	969
20.8.1	Initialization	969
20.8.2	Electric and Magnetic Field Updates	970
20.8.3	Boundaries	972
20.8.4	Source Excitation	974
20.8.5	Archiving Observation Nodes	975
20.8.6	Multipass Rendering	975
20.8.7	Display	977
20.9	Performance Measurements of the GPU Accelerator	977
20.10	Summary and Conclusions	978
	References	978
	Acronyms and Common Symbols	981
	About the Authors	985
	Index	997